Available online at www.sciencedirect.com
SCIENCE DIRECT
Polymer 46 (2005) 3163–3174
polymer
www.elsevier.com/locate/polymer

Structure, morphology and non-isothermal crystallization behavior of polypropylene catalloys

Qiang Zheng[a,c,*], Yonggang Shangguan[a], Shouke Yan[b], Yihu Song[a], Mao Peng[a], Qibin Zhang[a]

[a]*Department of Polymer Science and Engineering, Zhejiang University, Hangzhou 310027, People's Republic of China*
[b]*State Key Laboratory of Polymer Physics and Chemistry, Institute of Chemistry, Chinese Academy of Sciences, Beijing 100080, People's Republic of China*
[c]*State Key Laboratories of Chemical Engineering, Polymer Reaction Engineering Division, Zhejiang University, Hangzhou, 31007, People's Republic of China*

Received 10 September 2004; received in revised form 30 December 2004; accepted 27 January 2005
Available online 8 March 2005

Abstract

The structure, morphology and non-isothermal crystallization behavior of polypropylene catalloys (PP-cats) as well as pure polypropylene were investigated via differential scanning calorimeter (DSC), wide angle X-ray diffraction (WAXD) and real-time hot-stage optical microscopy (OM). The results reveal that the crystalline structures of PP-cats change with variations of the crystallization conditions and composition. The crystalline phase might consist of α-PP, β-PP and PE crystals. The content of β-PP increases with the increase of EP copolymer content and the cooling rate. At lower cooling rates, the morphologies of all non-isothermal crystallized PP-cats show spherulitic structure, and the decrease of crystal perfection and the increase of nucleation density of PP-cats system could be evidently observed. Considering the compositions of PP-cats, these indicated that the interactions between propylene homopolymer and the ethylene–propylene copolymers (both random and block ones) are in favor of the enhancement of the nucleation ability of α-form as well as β-form. In comparison with pure PP, the overall crystallization rates of the PP-cats increase dramatically, while the growth rates of the spherulites in all PP-cats decrease distinctly under the given cooling conditions. These experimental results were explained on the basis of diluting effect and obstructing effect on the mobility of PP chains in the ethylene–propylene copolymer.

Keywords: Polypropylene catalloys; Non-isothermal crystallization; Morphology

1. Introduction

Isotactic polypropylene (iPP) is a thermoplastic material widely used in several sectors, as it offers interesting combinations of good mechanical performance, heat resistance, fabrication flexibility and low cost. However, it has relatively poor impact resistance, especially at low temperatures. Therefore, a great deal of effort has been made to modify its mechanical properties through physical or chemical methods. In the past several decades various kinds of copolymers of PP and blends composed with various kinds of polymers and/or inorganic fillers have been developed. Meanwhile, the microstructures, crystallization behavior and their relation with the properties of the modified polypropylenes have been studied extensively by many researchers [1–25].

In recent years, a catalloys technology, or frequently referred to the in-reactor blending technology, was developed by Montell Company. This has opened up new horizons for polyolefin materials. The technology involves bulk polymerization of propylene and then gas-phase copolymerization of ethylene and propylene under the driving of spherical superactive $TiCl_4/MgCl_2$ based catalyst systems [26–29]. In comparison with traditional iPP blends prepared by mechanical blending with ethylene–propylene random copolymer (EPR) or ethylene–propylene–diene terpolymer (EPDM), ethylene–propylene random copolymer in in-reactor blends can reach a high degree of dispersion; hence they are called polypropylene catalloys (PP-cats) and present much higher impact strength [30,31]. The catalloys process endows a wider range of rubble content and a better control of the phase structure in the alloy, resulting in the possibilities to prepare materials with excellent mechanical properties.

* Corresponding author. Tel.: +86 571 8795 2522; fax: +86 571 8795 2522.
E-mail address: zhengqiang@zju.edu.cn (Q. Zheng).

0032-3861/$ - see front matter © 2005 Elsevier Ltd. All rights reserved.
doi:10.1016/j.polymer.2005.01.097

By means of temperature-gradient extraction fractionation, ^{13}C NMR, FTIR, DSC and WAXD, Fan et al. [29,32] has studied the composition of polypropylene catalloys and pointed out that PP-cats were mainly composed of propylene homopolymer, ethylene–propylene random copolymer and ethylene–propylene block copolymer with different PE and PP segmental length. It is understandable that the excellent mechanical properties of PP-cats are related to their crystallization behavior and structure differing from usual PP/EPR blends. However, the crystallization behavior of PP-cats based on spherical catalysts has seldom been reported [33]. The objective of the present article is to investigate the structure, morphology and the non-isothermal crystallization behavior of polypropylene catalloys with different compositions.

2. Experimental

2.1. Materials

The grade of polypropylene (isotactic homopolymer, $M_n = 80{,}643$ and $M_w = 333{,}465$) used in this study was T300, supplied by Sinopec Shanghai Petrochemical Co. of China.

PP-cats were kindly supplied by the Institute of Polymer Science of Zhejiang University of China. The synthesis of PP-cats included three steps, i.e., pre-polymerization of propylene, bulk polymerization of propylene, and gas-phase copolymerization of ethylene and propylene. The PP-cats were designated as PEP20, PEP30, PEP40, PEP50 and PEP60, respectively, in which capital E represents ethylene component and the numbers represent its percentage used in the gas-phase copolymerization in the third stage. The content of ethylene and ethylene–propylene copolymer in the catalloys and the melting flow indices (MFI) of these specimens are listed in Table 1.

2.2. Sample preparation

The iPP and PP-cats samples were prepared by compression-molding at 200 °C with a pressure of 10 MPa for 5 min. After the pressure was released, the molded samples were removed from the press and cooled down to room temperature.

Table 1
Characteristics of PP and PP-cats used

Sample	Content of ethylene (mol%)	Content of ethylene–propylene copolymer (wt%)	MFI (g/10 min)
IPP	–	–	3.00
PEP20	2.87	17.8	1.54
PEP30	3.10	19.9	1.38
PEP40	11.80	23.2	1.27
PEP50	17.80	30.0	–
PEP60	27.10	34.2	0.56

2.3. Differential scanning calorimetry (DSC)

A Perkin–Elmer series 7 differential scanning calorimeter (DSC) with nitrogen as purge gas was used to investigate the crystallization behavior of the iPP and PP-cats. Pure indium and zincum were used as reference materials to calibrate both the temperature scale and the melting enthalpy before the samples were tested. The samples (about 5.0 mg) were heat-treated at 200 °C for 10 min to eliminate the thermal history, and then cooled down to 30 °C at constant cooling rates of 2, 5, 10, 20 and 40 °C/min, respectively.

The time corresponding to the intersection between the extrapolation of the DSC curves after and before crystallization was used as the beginning of crystallization [34]. The relative crystallinity developed on cooling to temperature T was defined as the fractional area confined between the rate time curve and the baseline on the measured DSC exotherm. The temperatures were corrected for thermal lag between the samples and the calorimeter furnace using a calibration technique employing pure indium.

The percentage of β-PP crystals for a sample, ϕ_β, was determined by the relative crystallinity of α- and β-PP according to Eq. (1) as given in Ref. [34]

$$\phi_\beta = \frac{X_\beta}{X_\alpha + X_\beta} \times 100\% \tag{1}$$

where X_α and X_β are the crystallinity of the α-phase and β-phase, respectively, based on specific fusion heats of the samples.

Considering the coexistence of α- and β-PP crystals in the treated samples, the crystallinity of each phase has been calculated separately according to Eq. (2) as given as

$$X_i = \frac{\Delta Hi}{\Delta H_i^\theta} \times 100\% \tag{2}$$

where ΔH_i is the calibrated specific fusion heat of either α- or β-PP crystal, while ΔH_i^θ is the standard fusion heat of either α- or β-PP crystals, which is 178 J/g for α-phase and 170 J/g for β-phase [35].

The DSC curves of some samples exhibited both α- and β-fusion peaks. The specific fusion heats for α- and β-phase were determined according to the following calibration method. The total fusion heat, ΔH, was integrated from 90 to 180 °C on the DSC thermogram. A vertical line was drawn through the minimum between the α- and β-fusion peaks and the total fusion heat was divided into β-component, ΔH_β^*, and α-component, ΔH_α^*. Since the less-perfect α-crystals melt before the maximum point during heating and gave rise to some contributions to the ΔH_β^*, the true value of β-fusion heat, ΔH_β, has been approximated by a production of multiplying ΔH_β^* with a calibration factor A [36]:

$$\Delta H_\beta = A \times \Delta H_\beta^* \tag{3}$$

$$A = \left[1 - \frac{h_2}{h_1}\right]^{0.6} \quad (4)$$

$$\Delta H_\alpha = \Delta H - \Delta H_\beta \quad (5)$$

2.4. Optical microscopy (OM)

For optical microscopy observation, an Olympus BH-2 optical microscope (OM) equipped with a homemade hot stage and a CCD color camera was used in this study. The samples sandwiched between two microscope cover slips were first heated to 200 °C for 10 min to erase its thermo-mechanical prehistory, and then cooled from the melt down to room temperature (about 25 °C) at constant rates, ranging from 0.5 to 5 °C/min. For performing isothermal crystallization of pure iPP at crystallization temperatures ranging from 126 to 134 °C, the iPP melts were quickly transformed to another hot stage with a chosen crystallization temperature. Dry nitrogen gas was purged through the hot stage in all heating and cooling processes.

The crystallization processes were in situ observed and the morphologies were recorded at constant time intervals. All images presented in this work were taken under the crossed-polarized condition. The diameters of a series of spherulites grown for different periods of times were measured and the spherulite growth rates, G, were calculated using the procedure proposed by Chen and Chung for solidification performed during cooling at a constant cooling rate [37]. Reported results for spherulite growth rate were averages of at least five measurements. The precision of controlled hot-stage is less than ± 1.0 °C.

2.5. Wide angle X-ray diffraction

Wide-angle X-ray diffraction (WAXD) patterns were obtained using a Rigaku D/max-IIIB diffractometer with the Cu Kα radiation at room temperature. The operating condition of the X-ray source was set at a voltage of 40 kV and a current of 300 mA in a range of $2\theta = 0$–$50°$.

3. Results

As mentioned in the introduction part, PP-cats consist mainly of propylene homopolymer, ethylene–propylene random copolymer and ethylene–propylene block copolymer with different PE and PP segmental length. It is well-known that the propylene homopolymer is one of the semicrystalline polymers exhibiting pronounced polymorphic crystalline modifications designated as monoclinic α, trigonal (or frequently hexagonal) β, and orthorhombic γ forms [38–40]. The ethylene–propylene random copolymer can hardly crystallize, while ethylene–propylene block copolymer may crystallize depending upon the PE and PP segmental length. Consequently, the microstructures of various PP-cats may be influenced not only by the crystallization conditions, but also the compositions.

3.1. Melting behavior

The DSC melting traces of the pure PP and various catalloys specimens crystallized at various cooling rates are shown in Fig. 1. Obviously, the melting traces of all specimens crystallized at cooling rate of 2 °C/min demonstrate single melting peak around 160 °C. For pure PP, the melting peak shifts to lower temperature with the increase of cooling rates, and a shoulder peak appears at higher cooling rate than 10 °C/min. For PP-cats, however, one or two peaks appear at about 144–150 °C on the melting traces when the samples were prepared with a cooling rate faster than 5 °C/min. These peaks seem to strengthen with the increase of ethylene content in the catalloys. Moreover, for the PEP60, a third melting peak appears at about 120 °C under all sample preparation conditions.

3.2. Optical microscopy study

It was documented that PP/ethylene–propylene random copolymer is an immiscible system and the ethylene–propylene copolymer disperses better in the PP-cats than conventional polypropylene/ethylene–propylene rubber blends prepared by mechanical blending [32]. Optical microscopic observation demonstrates that for all PP-cats under investigation, no obvious segregated domains in the melt can be observed at 200 °C by using optical microscope. This implies that the domain dimension of the dispersed phases is below the resolution obtainable by optical microscopy. With the decrease of the temperature, the morphology changes remarkably because a liquid–solid phase separation resulting from the PP crystallization takes place at T_c. It should be pointed out that the remaining amorphous phase is visibly homogeneous under optical microscope after new phases (PP crystalline phase) form through crystallization. Fig. 2 shows the morphologies of various PP-cats as well as pure PP crystallized at cooling rate of 2 °C/min. It can be seen that the morphologies of the specimens crystallized from the melts are always spherulitic. Even for the PP-cats PEP60, though it is very difficult to distinguish the shape of spherulites, the in situ optical microscopy observation shows, however, the formation and quick impingement of the small spherulites resulting from too many nuclei. The number of spherulites and their dimension depend strongly on composition. While the spherulite size decreases, the number of spherulites increases generally with the increase of the ethylene content in PP-cats. Moreover, with careful inspection, it can be concluded that the spherulitic structure becomes more deficient with the increase of ethylene contents in the PP-cats. All these results clearly indicate that the existence of ethylene–propylene random and block ethylene–propylene copolymers has influenced the crystallization morphologies of PP.

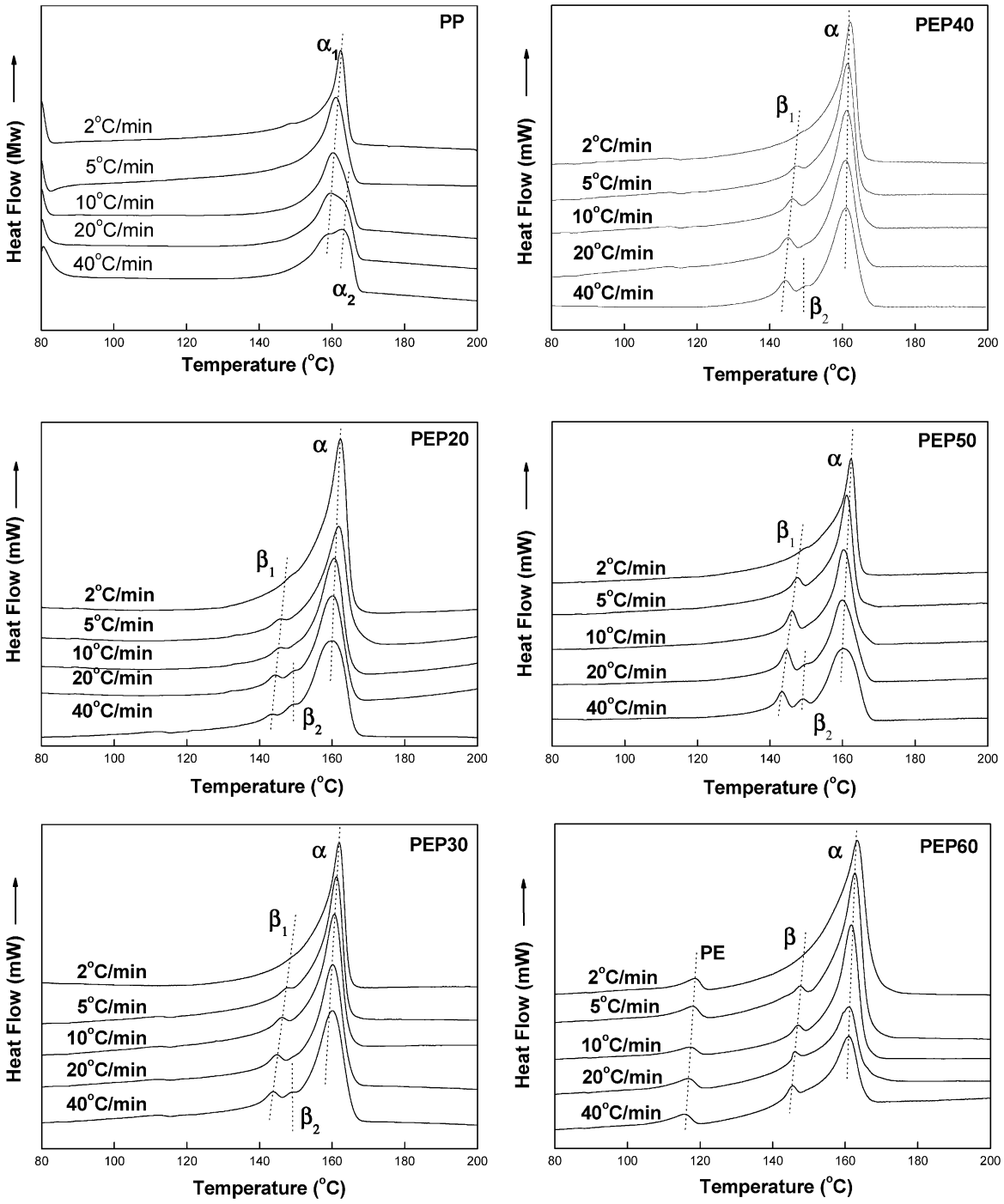

Fig. 1. DSC melting traces of iPP and various PP-cats prepared with different cooling rates (scanning rate: 10 °C/min).

The spherulites observed through birefringence measurements exhibit basically an optical positive character for all samples (both pure PP and PP-cats), reflecting the formation of the most common α-iPP modification. It should be noted that the birefringence of the PP-cats is much weaker than that of the pure PP, meaning there exists the influence of ethylene–propylene random copolymer and ethylene–propylene block copolymers on the crystalline structure of PP-cats. On the other hand, a few of randomly dispersed microdomains in the optical micrographs of PEP50 and PEP60, as indicated by white arrows, are colorful even without using the λ plate and exhibit very strong negative birefringence. These are the characteristic natures of the β-form iPP. Melting test demonstrates that these domains melt at about 150 °C, while the rest areas melt at about 160 °C (see Fig. 3). This unambiguously indicates the formation of some crystalline β-iPP randomly dispersed in the predominant α-iPP.

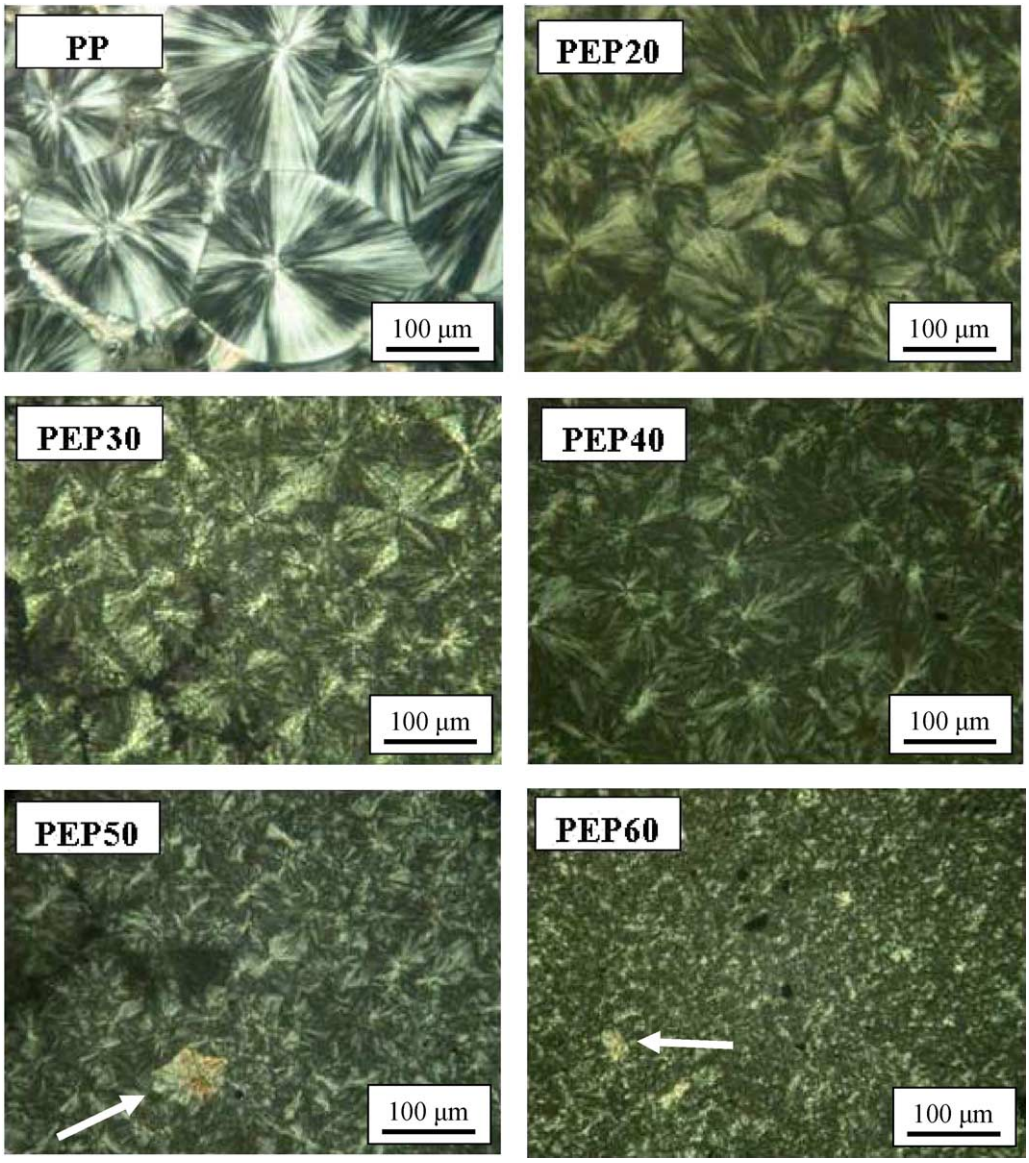

Fig. 2. Optical micrographs of iPP and PP-cats crystallized at cooling rate of 2 °C/min. The white arrows in the pictures indicate the β-iPP (crossed polars).

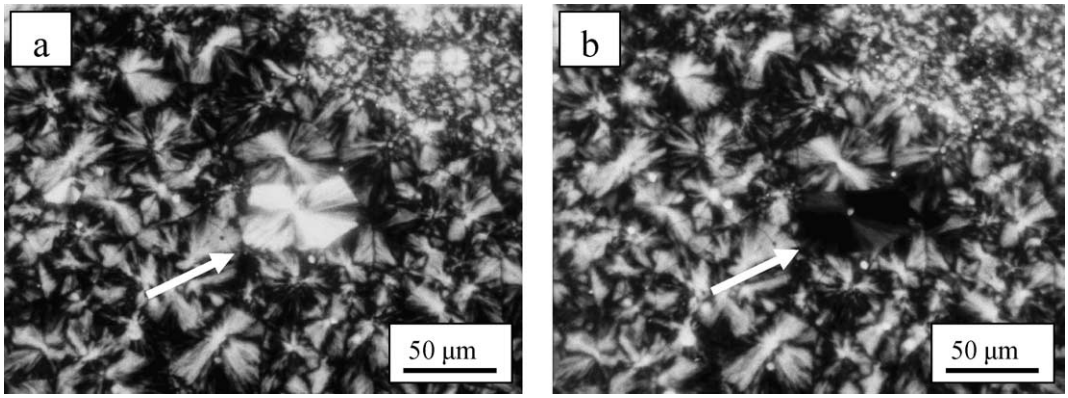

Fig. 3. Optical micrographs of the β-PP spherulite in PEP50 specimens taken during heating from the room temperature to melting temperature at (a) 145 °C and (b) 155 °C (heating rate: 10 °C/min). The white arrows in the pictures indicate the β-iPP (crossed polars).

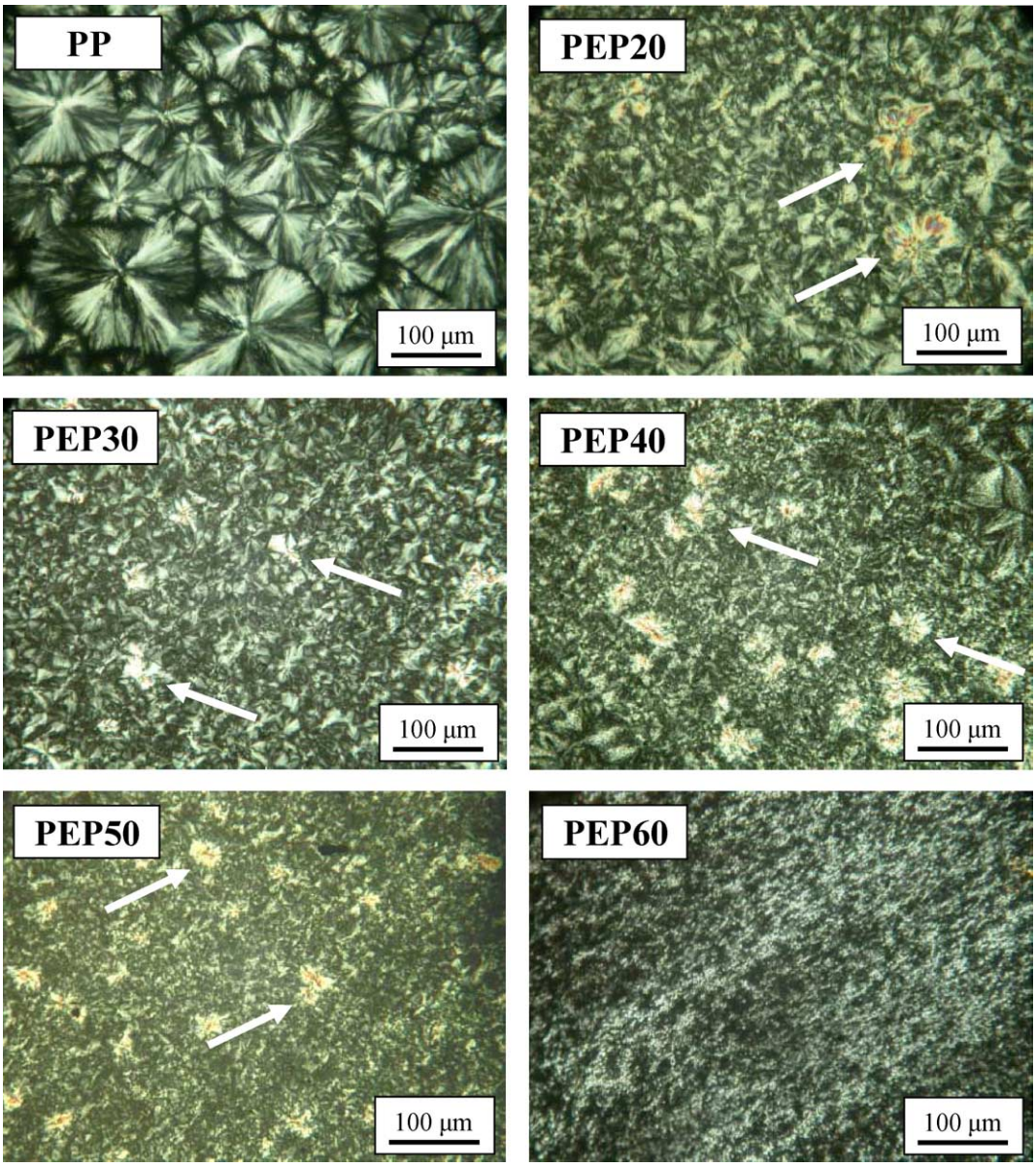

Fig. 4. Optical micrographs of iPP and PP-cats crystallized at cooling rate of 5 °C/min. The white arrows in the pictures indicate the β-iPP (crossed polars).

With the increase of the cooling rate during sample preparation, the morphology changes somewhat. Fig. 4 shows a series of optical micrographs of the PP and PP-cats crystallized during the cooling process at 5 °C/min. The spherulites of various PP-cats and pure PP present still basically the positive birefringence. However, the colorful domains with strong negative birefringence, i.e., the β-iPP crystals, are now no more the special case of PEP50 and PEP60 rather than a common feature of all PP-cats, as indicated by the white arrows in Fig. 4. The number of the β-PP domains of the PEP50 is much more than that generated by cooling the sample at 2 °C/min, indicating an increase of β-PP content in crystalline phase of PEP50 with increasing cooling rate. Moreover, the content of β-PP increases with increasing ethylene content in the PP-cats. It can be further seen from Fig. 4 that the crystalline spherulites of PP-cats as well as pure PP are more irregular than those formed at a cooling rate of 2 °C/min.

3.3. WAXD analysis

To find out the exact crystalline structure of the PP-cats, WAXD was performed. Fig. 5 shows the WAXD spectra of the specimens crystallized at cooling rates of 2 and 5 °C/min, respectively. It can be seen from Fig. 5(a) that all of the most intense WAXD reflections at 2θ angles of 14.0, 16.8, 18.6, 21.2 and 21.9°, corresponding to the (110), (040), (130), (111) and $(13\bar{1})$ lattice planes of the most common α-monoclinic structures, have appeared in the X-ray diffraction spectra of every sample. This clearly indicates

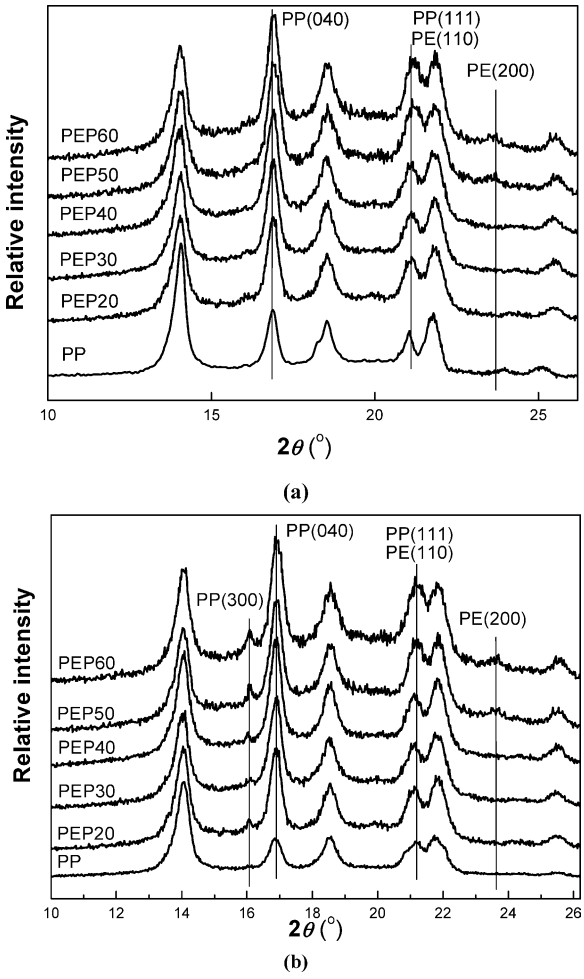

Fig. 5. WAXD patterns of PP and PP-cats crystallized at different cooling rates. (a) 2 °C/min and (b) 5 °C/min.

that in all cases the iPP crystals grow dominatingly in their monoclinic α-modification. For the PP-cats having a high PE content, e.g., PEP50 and PEP60, there exists an extra reflection at 2θ of 24.0°. This reflection corresponds to the (200) lattice planes of the PE crystals and may imply the existence of the PE crystals. The most intense (110) diffraction of PE overlaps with the (111) reflection of α-PP, as indicated in Fig. 5(a). Compared with its neighborhood peak, the change in intensity of this peak demonstrates the existence of the strong $(110)_{PE}$ reflection. Based on this result, it can be concluded that the ethylene segment in ethylene–propylene block copolymers with high ethylene content, such as PEP50 and PEP60, is long enough to crystallize independently. In Fig. 5(b), another peak appears at 2θ of 16.0°, which can be accounted for by the (300) lattice planes of the hexagonal β-PP [39,40]. There may be also the characteristic (301) β-PP reflection at 21.2°, which overlaps with the (111) of α-PP as well as (110) of PE. The appearance of $(300)_{\beta PP}$ indicates the existence of β-PP crystals in the PP-cats specimens crystallized at cooling rates of 5 °C/min. Moreover, the increase in intensity of the $(300)_{\beta PP}$ indicates that the β-PP content increases with the increase of ethylene content in the PP-cats. This is in good accordance with the results by optical microscopy observation.

The total crystallinity and β-PP content of the studied samples obtained from DSC data are listed in Table 2. It can be clearly seen that the total crystallinity of pure PP and various PP-cats specimens decreases generally with the increase of cooling rate. On the contrary, the β-PP content, as plotted in Fig. 6, increases remarkably with the increase of cooling rate until 20 °C/min. The β-PP content of various PP-cats specimens crystallized at 40 °C/min approximates to that of 20 °C/min. Furthermore, the increases of ethylene content in PP-cats also result in the decrease of the total crystallinity and the increase of the β-PP content. This implies that the existences of ethylene–propylene random copolymer and ethylene–propylene block copolymer go against the crystallization of whole PP-cats system, whereas they facilitate the formation of β-PP crystals.

3.4. Crystallization kinetics

The crystal growth rate, G, was measured for the isothermal and non-isothermal crystallization process, while the overall crystallization rate was obtained from the non-isothermal DSC data. Fig. 7 presents the plots of spherulite growth rates of pure iPP as a function of temperature under different cooling rates as well as different isothermal crystallization conditions. Obviously, the spherulite growth rate of pure PP increases with the decrease of crystallization temperature at all conditions under investigation. It can be further seen that the spherulite growth rates measured for the non-isothermal and isothermal crystallization processes are in good agreement and fit well in the same curve.

The spherulite growth rates of various PP-cats are also plotted as the function of crystallization temperature in Fig. 8. It is easily seen that the spherulite growth rates of all PP-cats specimens is distinctly lower than the pure PP, especially in the lower temperature range. Nevertheless, they exhibit a similar temperature-dependence as pure PP,

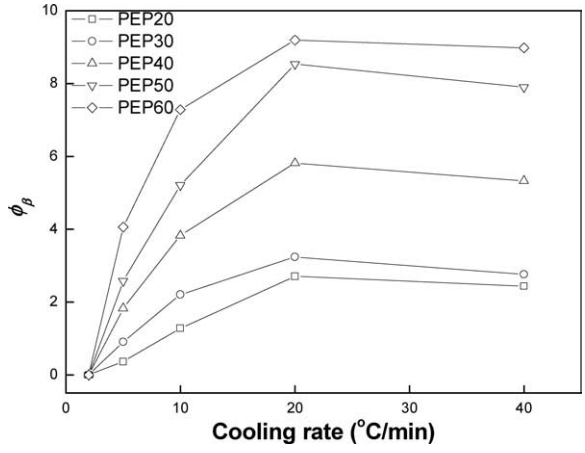

Fig. 6. Dependence of β-crystal content in various PP-cats on cooling rate.

Table 2
Overall crystallinity and the β-PP content in pure PP and PP-cats crystallized at different cooling rates

Cooling rate (°C/min)	PP		PEP20		PEP30		PEP40		PEP50		PEP60	
	Xc (%)	ϕ_β (%)	Xc (%)	ϕ_β (%)	Xc (%)	ϕ_β (%)	Xc (%)	ϕ_β (%)	Xc (%)	ϕ_β (%)	Xc (%)	ϕ_β (%)
2	53.13	–	46.33	0	40.22	0	36.27	0	32.96	0	28.70	0
5	51.17	–	42.80	0.37	37.53	0.91	34.11	1.83	30.42	2.58	27.04	4.06
10	50.86	–	36.06	1.28	34.39	2.21	31.31	3.83	28.12	5.21	25.01	7.28
20	49.19	–	32.20	2.71	29.18	3.24	28.52	5.82	25.85	8.54	23.62	9.19
40	47.93	–	30.55	2.44	28.84	2.76	27.22	5.33	23.17	7.90	22.12	8.98

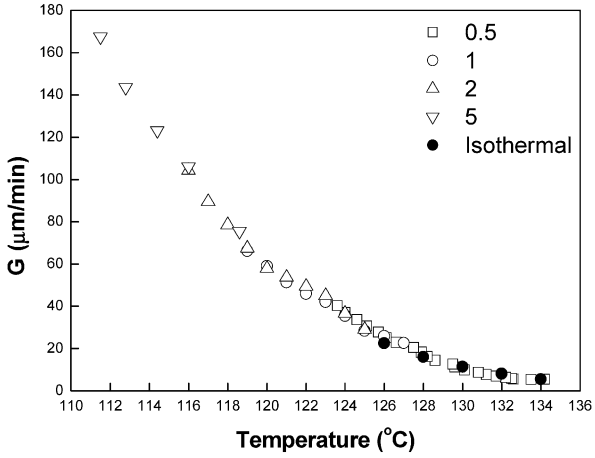

Fig. 7. Spherulite growth rate data of pure PP measured isothermally and at several cooling rates.

i.e., increase with the decrease of crystallization temperature. These results are in good accordance with the results concerning spherulite growth rate of PP blend [13,19,20,24], and also, they show a composition dependence of spherulite growth rate in PP-cats. With the increase of the ethylene content, the spherulite growth rate decreases. This behavior is more obvious when the ethylene-content in PP-cats is lower than 11.8 mol%, meaning that the thermal condition exerts less effect on spherulite growth rate of PP-cats with higher ethylene content.

It is well-known that the half-time of crystallization, $\tau_{1/2}$, is another very important parameter describing the overall crystallization rate. The $\tau_{1/2}$ obtained for pure PP and PP-cats specimens are plotted against cooling rate in Fig. 9. It should be mentioned that the $\tau_{1/2}$ of PEP60 is calculated without taking the crystallization of PE into account. It can be clearly seen from Fig. 9 that the $\tau_{1/2}$ of pure PP is higher than that of any PP-cats specimen at all cooling rates used, peculiarly at lower cooling rates. The $\tau_{1/2}$ decreases with the increase of ethylene content. These results demonstrate that

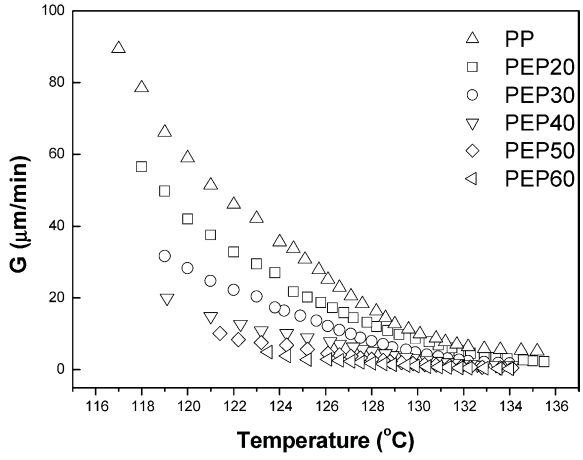

Fig. 8. Spherulite growth rate data of pure PP and PP-cats as a function of crystallization temperature.

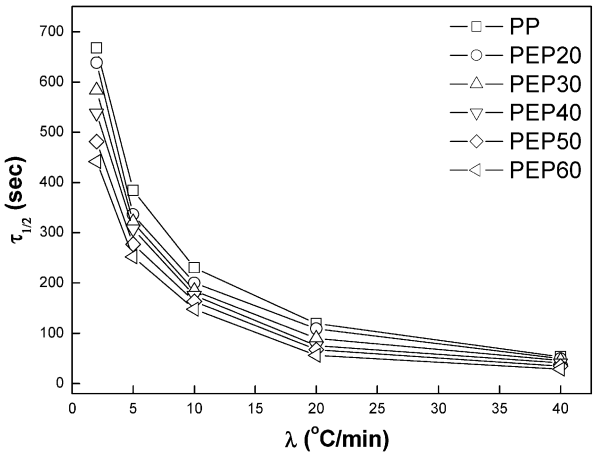

Fig. 9. Half time of crystallization, $\tau_{1/2}$, vs. cooling rates, λ, for PP and various PP-cats specimens.

the overall crystallization rate of PP-cats, which is dependent on the ethylene content, is faster than pure PP. This is in agreement with the previous report on isothermal crystallization of PP-cats [33].

Representative crystallization exotherms of polypropylene catalloys PEP20 and PEP60 at several cooling rates are shown in Fig. 10. Except for the appearance of the PE crystallization peak for PEP60, the non-isothermal crystallization processes of PEP20 and PEP60 exhibit the same dependence on cooling rate, i.e., the crystallization exotherms of PP-cats shift to lower temperature with the increase of the cooling rate. Comparing parts A with B in Fig. 10, we can further conclude that the crystallization exotherms of PP-cats shift to higher temperature with the increase of the ethylene content. The onset and peak crystallization temperatures (T_b and T_p, respectively) of pure PP and PP-cats were plotted against cooling rate. As shown in Fig. 11, the T_b for PP-cats is higher than that of pure PP at all cooling rates, indicating the crystallization of PP-cats starts earlier than that of pure PP. Especially, T_b of PEP60 at various cooling rates is considerably high, whereas the difference of onset temperatures between other PP-cats is small. It is believed that ethylene–propylene copolymer acts as nucleation agent in the PP-cats and the results are related to the degree of disperse of ethylene–propylene random copolymer. Similarly, the T_p depends also remarkably on the cooling rate and composition of PP-cats (see Fig. 12). An obvious increase of T_p is observed with the increase of ethylene content in PP-cats and decrease of cooling rate. These changes are consistent with the variation of overall crystallization rate of PP-cats.

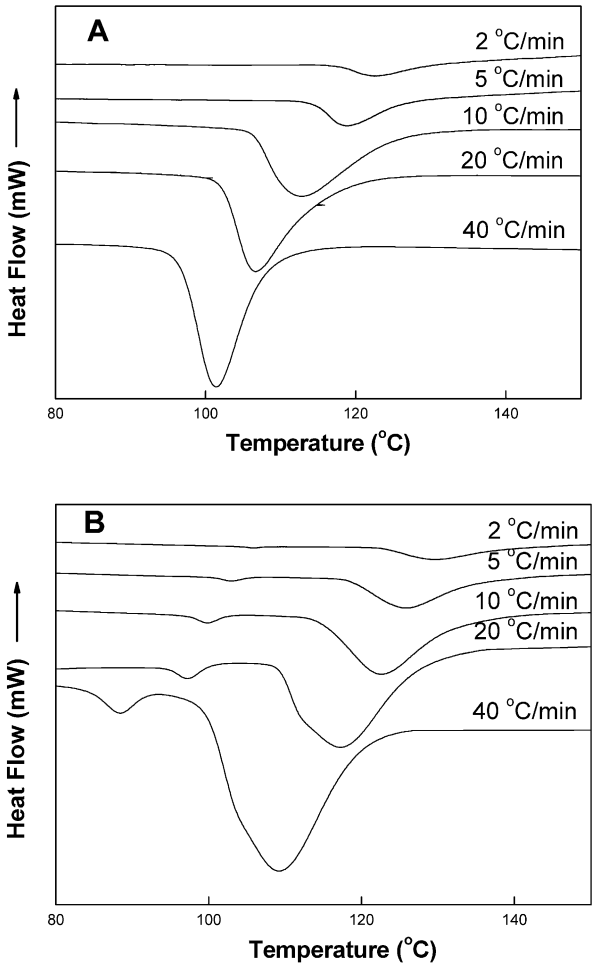

Fig. 10. DSC crystallization exotherms of (A) PEP20 and (B) PEP 60 crystallized at different cooling rates.

4. Discussion

4.1. Multiple melting behaviors of PP-cats

The multiple melting behavior of pure PP sample, which depends on thermal conditions of crystallization, has been reported by many researches [41–44]. Petracone et al. reported that the existing of less-ordered α_1 and more-ordered α_2 forms with a well-defined deposition of up and down helices in the unit cells could result in the double

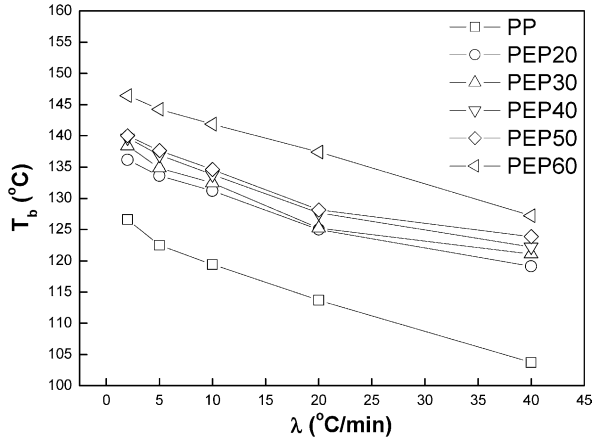

Fig. 11. Dependence of crystallization onset temperature for pure PP and PP-cats on cooling rate.

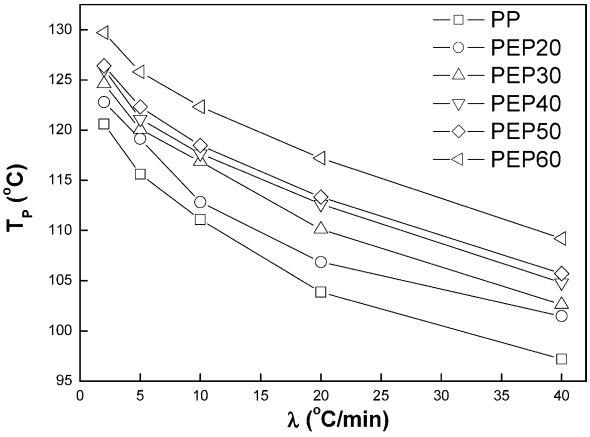

Fig. 12. Dependence of maximum crystallization peak for pure PP and PP-cats on cooling rate.

melting peaks [41–43]. The existence of two phases, α_1 and α_2 for PP was confirmed using SAX and DSC techniques [44]. Thus, in Fig. 1, the double melting peaks of pure PP, α_1 and α_2 indicate the existence of α-crystal with different structures at higher cooling rates.

According to the experimental results mentioned above, taking the WAXD results into account, the melting peak at about 120 °C of PEP60 doubtless reflects the melting of PE crystals and has nothing to do with PP. It should be noted that there might exist also some PE crystals in other PP-cats samples, e.g., PEP50, as can be deduced from the results by WAXD. Their amounts are, however, not enough to be differentiated under DSC measurement. On the other hand, the peaks at about 144–150 °C should be associated with the melting of β-modification of PP, The existence of which has also been confirmed by both optical microscopic and WAXD. As shown in Fig. 1, two melting peaks, β_1 and β_2 were observed at higher cooling rates in PP-cats. It accords with the literatures that the multiple melting peaks of β-PP might exist in the temperature of 141–152.5 °C [36,45]. Therefore, the double β-melting peaks present the existence of β-PP with different crystalline perfection. It is worth noting that the optical microscopy observation illustrates the existence of β-PP in PEP50 and PEP60 with cooling rate of 2 °C/min. This has, however, not been identified in the WAXD experiments. This is understandable that the optical microscope concerns the supermolecular structure of the individual microdomains, while the WAXD reflects the overall crystalline structure of the sample. As a result, some crystalline structure of the minority crystalline phase could be covered up by the majority phase.

4.2. The formation mechanism of β-PP

It was well documented that the monoclinic α-PP, the thermodynamically most stable crystalline form, can be easily generated by melt crystallization. The nucleation of metastable β-form occurs much more rarely in bulk crystallization than that of the predominant α-modification. Nevertheless, both α- and β-PP crystals could coexist under several crystallization conditions, and the proportion of these two phases depends strongly on the thermal conditions and the way of nucleation [38–40,45–52]. Studies on the blends of PP with various copolymers demonstrate that copolymer components, such as ethylene-propylene copolymer (EPR) [1] and ethylene–propylene–diene terpolymer (EPDM) [7], are in favor of the formation of β-PP crystals. It was suggested that the formation of β-PP in these cases results from the effect of the impact modifier on the nucleation. Some systematic studies have been reported that the formation of β-iPP supermolecular structure can be promoted for the sheared polymer melts in a certain temperature range [51–56]. More recently, it is suggested by the author [57,58] that the orientation status of the PP chains in melting state plays a leading role in generating the β-iPP. At the present case, taking the fact into consideration that β-PP has been generated in PP-cats rather than pure PP under the same crystallization conditions, the formation of β-PP in PP-cats should result from the cooperative interaction between PP homopolymer and the ethylene–propylene copolymers (both random and block ones). As the ethylene–propylene random copolymer cannot crystallize and the PE segments cannot co-crystallize with the PP segments, it is reasonable to assume that chain orientation of PP to some extent may be induced by the phase separation. Therefore, it is suggested that the formation of β-PP here is also orientation induced. Considering that the phase-separation process depends unambiguously on the thermal conditions, the content of β-PP is closely related the cooling rates given.

4.3. Crystallization kinetics of PP-cats

The final one concerns the crystallization kinetic of the PP-cats. It is clear that the overall crystallization rate increases when compared to pure PP, while the spherulitic growth rate decreases. Furthermore, the overall crystallization rate continuously increases while the spherulitic growth rate decreases with the increase of EP content. This is quite different from those for most of the polypropylene blends, where the overall crystallization rate decreases due to the addition of impurity [8,11–13]. Arroyo et al. [59] reported that EPDM particles acting as nucleating agent increased the crystallization rate and crystallinity of the PP at lower EPDM contents ($\leq$25%) in PP/EPDM blend, but the crystallization rate decreased with the increase of EPDM composition at higher percentages. All these show that crystallization kinetics of PP-cats is different from the usual PP/EPR or PP/EPDM blends prepared by mechanical blending. This may result from the cooperation of the higher nucleation density and lower crystallinity in PP-cats. Moreover, the studies on spherulite growth rates of polymer blends show that the spherulite growth rates of polymer blends without evident phase-separation are generally slower than those of pure crystalline polymers, whereas

the spherulite growth rates of polymer blends after phase-separation are seldom affected by the second component [24]. Consequently, concerning the better disperse of ethylene–propylene copolymer in PP matrix, the decrease of spherulite growth rate for PP-cats can be explained by the diluting effect of ethylene–propylene copolymer [19,20,24] and obstructing effect on the mobility of PP chains [59].

5. Conclusions

The structure, morphology and crystallization behavior of PP-cats as well as pure polypropylene were investigated. The results reveal that the crystalline structure of PP-cats changes with the variation of the crystallization conditions and compositions. There exist three crystalline phases, i.e., α-PP, β-PP and PE crystals, for PEP60 at any given thermal conditions, while only α- and β-PP phases were detected for other PP-cats at faster cooling rates. The formation of β-PP may result from some kind of chain orientation in the melts induced by phase-separation. The existence of two kinds of ethylene–propylene copolymers, random and block copolymers, results in an increase of the overall crystallization rate while a decrease of the spherulite growth rate under the given cooling conditions. On the other hand, the increase of the overall crystallization rate may be explained in view of the strong nucleation ability of the EP copolymers on the PP-cats, while the decrease of the spherulite growth rate can be explained on the basis of the diluting effect and obstructing effect on the mobility of PP chains in the ethylene–propylene copolymer.

Acknowledgements

It is grateful for the financial supports of the National Natural Science Fund for Distinguished Young Scholars (No. 50125312), Key Program of National Science Foundation of China (No. 50133020) and National Natural Science Foundation of China (No. 50373037).

References

[1] Karger-Kocsis J, Kallo A, Szafner A, Bodor G. Polymer 1979;20:37.
[2] Stehling FC, Huff T, Speed CS, Wissler G. J Appl Polym Sci 1981;26:2693.
[3] Gan SN, Burfield DR, Soga K. Macromolecules 1985;18:2684.
[4] Inaba N, Sato K, Suzuki S, Hashimoto T. Macromolecules 1986;19:1690.
[5] Inaba N, Yamada T, Suzuki S, Hashimoto T. Macromolecules 1988;21:407.
[6] Coppola F, Greco R, Martuscelli E, Kammer HW, Kummerlowe C. Polymer 1987;28:47.
[7] Ha CS, Kim SC. J Appl Polym Sci 1988;35:2211.
[8] Besombes M, Menguei JF, Delmas G. J Polym Phys, Part B: Polym Phys 1988;26:1881.
[9] Monasse B, Haudin JM. Colloid Polym Sci 1988;266:679.
[10] Wang LX, Huang BT. J Polym Phys, Part B: Polym Phys 1990;28:937.
[11] Orazio L, Mancarella C, Martuscelli E, Sticotti G. Polymer 1993;34:3671.
[12] Lee CH, Saito H, Inoue T. Macromolecules 1995;28:8096.
[13] Avalos F, Lopez-Manchado MA, Arroyo M. Polymer 1996;37:5681.
[14] Weimann PA, Jones TD, Hillmyer MA, Bates FS, Londono JD, Melnichenko Y, et al. Macromolecules 1997;30:3650.
[15] Triolo A, Silvestre C, Cimmino S, Martuscelli E, Caponetti E, Triolo R. Polymer 1998;39:1697.
[16] Blom HP, Teh JW, Bremner T, Rudin A. Polymer 1998;39:4011.
[17] Thomann Y, Suhm J, Thomann R, Bar G, Maier RD, Mülhaupt R. Macromolecules 1998;31:5441.
[18] Seki M, Nakano H, Yamauchi S, Suzuki J, Matsushita Y. Macromolecules 1999;32:3227.
[19] Silvestre C, Cimmino S, Alma ED, Di Lorenzo ML, Di Pace E. Polymer 1999;40:5119.
[20] Di Lorenzo ML, Cimmino S, Silvestre C. Macromolecules 2000;33:3828.
[21] Opdahl A, Phillips RA, Somorjia GA. Macromolecules 2002;35:4387.
[22] Silvestre C, Cimmino S, Pirozzi B. Polymer 2003;44:4273.
[23] Schönherr H, Waymouth RM, Frank CW. Macromolecules 2003;36:2412.
[24] Di Lorenzo ML. Prog Polym Sci 2003;28:663.
[25] Tabtiang A, Phochalam N, Venables R. J Polym Phys, Part B: Polym Phys 2004;42:965.
[26] Wang LX, Huang BT. J Polym Sci, Part B: Polym Phys 1990;28:937.
[27] Galli P, Haylock JC. Makromol Chem Macromol Symp 1992;63:19.
[28] (a) Cai HJ, Luo XL, Ma DZ, Wang JM, Tan HS. J Appl Polym Sci 1999;71:93.
(b) Cai HJ, Luo XL, Ma DZ, Wang JM, Tan HS. J Appl Polym Sci 1999;71:103.
[29] Xu JT, Feng LX, Yang SL, Wu YN, Yang YQ, Kong XM. Polymer 1997;38:4381.
[30] Creco R, Mancarella C, Martuscelli E, Ragosta G. Polymer 1987;28:1929.
[31] Fu Z, Fan ZQ, Zhang YQ, Feng LX. Eur Polym J 2003;39:795.
[32] Fan ZQ, Zhang YQ, Xu JT, Wang HT, Feng LX. Polymer 2001;42:5559.
[33] Lin ZH, Peng M, Zheng Q. J Appl Polym Sci 2004;93:877.
[34] Mubarak Y, Harkin-Jones EMA, Martin PJ, Ahmad M. Polymer 2001;42:3171.
[35] Li JX, Cheung WL, Jia D. Polymer 1999;40:1219.
[36] Li JX, Cheung WL. Polymer 1998;39:6935.
[37] Chen M, Chung CT. J Polym Sci, Part B: Polym Phys 1998;36:2393.
[38] (a) Padden FJ, Keith HD. J Appl Phys 1959;30:1479.
(b) Padden FJ, Keith HD. J Appl Phys 1959;30:1485.
(c) Padden FJ, Keith HD. J Appl Phys 1966;37:4013.
(d) Padden FJ, Keith HD. J Appl Phys 1973;44:1217.
[39] Samuels RJ, Yee RY. J Polym Sci, A-2 1972;10:385.
[40] Turner-Jones A, Aizlewood J, beckett D. Makromol Chem 1964;75:134.
[41] Guerra G, Petracone V, Corradini P, De Rossa C, Napolitano R, Pirozzi B. J Polym Sci, Polym Phys Ed 1984;22:1029.
[42] Petracone V, Guerra G, De Rossa C, Tuzu A. Macromolecules 1985;18:813.
[43] Petracone V, Guerra G, De Rossa C, Tuzu A. Macromol Chem Rapid Commun 1984;5:631.
[44] Janimic JJ, Cheng SZD, Zhang A, Hsieh ET. Polymer 1992;33:728.
[45] Grein C, Plummer CJG, Kausch HH, Germain Y, Beguelin Ph. Polymer 2002;43:3279.
[46] Turner-Jones A, Cobbold AJ. J Polym Sci 1968;6:539.
[47] Norton DR, Keller A. Polymer 1985;26:704.
[48] Lovinger AJ, Chua JO, Gryte CC. J Polym Sci, Polym Phys Ed 1977;15:641.
[49] Garbarczyk J, Paukzta D. Polymer 1981;22:562.
[50] Lotz B, Fillon B, Therry A, Wittmann JC. Polym Bull 1991;25:101.

[51] Varga J. J Thermal Anal 1989;35:1891.
[52] Varga J. J Mater Sci 1992;27:2557.
[53] Varga J, Karger-Kocsis J. Polym Bull 1993;30:105.
[54] Varga J, Karger-Kocsis J. Polymer 1995;36:4877.
[55] Varga J, Karger-Kocsis J. J Mater Sci Lett 1994;13:1069.
[56] Varga J, Karger-Kocsis J. J Polym Sci, Polym Phys 1996;34:657.
[57] Li H, Jiang S, Wang J, Wang D, Yan S. Macromolecules 2003;36: 2802.
[58] Li H, Zhang X, Kuang X, Wang J, Wang D, Li L, et al. Macromolecules 2004;37:2847.
[59] Arroyo M, Zitzumbo R, Avalos F. Polymer 2000;41:6351.